Effects of autoclaving, EtOH and UV sterilization on the chemical, mechanical, printability and biocompatibility characteristics of alginate

Parth Chansoria^{1,2}, Lokesh Karthik Narayanan^{1,2,4}, Madison Wood^{3,5}, Claudia Alvarado^{1,2},

Annie Lin^{1,2} and Rohan A. Shirwaiker^{1,2,3,*}

- ¹ Edward P. Fitts Department of Industrial and Systems Engineering, North Carolina State University, Raleigh, NC 27695-7906, United States of America
- ² Comparative Medicine Institute, North Carolina State University, Raleigh, NC 27606, United States of America
- ³ Joint Department of Biomedical Engineering, University of North Carolina at Chapel Hill and North Carolina State University, Raleigh, NC 27695, United States of America
- ⁴ Department of Industrial and Manufacturing Engineering, North Dakota State University, Fargo, ND 58105, United States of America
- ⁵ Department of Mechanical and Aerospace Engineering, North Carolina State University, Raleigh, NC 27695, United States of America
- * Author to whom correspondence should be addressed (Email: rashirwaiker@ncsu.edu)

Abstract

Sterilization is a necessary step during the processing of biomaterials, but it can affect the materials' functional characteristics. This study characterizes the effects of three commonly used

sterilization processes – autoclaving (heat-based), ethanol (EtOH; chemical-based), and ultraviolet (UV; radiation-based) – on the chemical, mechanical, printability and biocompatibility properties of alginate, a widely used biopolymer for drug delivery, tissue engineering and other biomedical applications. Sterility assessment tests showed that autoclaving was effective against Grampositive and Gram-negative bacteria at loads up to 10⁸ CFU/ml, while EtOH was the least effective. Nuclear magnetic-resonance spectroscopy showed that the sterilization processes did not affect the monomeric content in the alginate solutions. The differences in compressive stiffness of the three sterilized hydrogels were also not significant. However, autoclaving significantly reduced the molecular weight and polydispersity index, as determined via gel permeation chromatography, as well as the dynamic viscosity of alginate. Printability analyses showed that the sterilization process as well as the extrusion pressure and speed affected the number of discontinuities and spreading ratio in printed and crosslinked strands. Finally, human adipose-derived stem cells demonstrated over 90% viability in all sterilized hydrogels over 7 days, but the differences in cellular metabolic activity in the three groups were significant. Taken together, the autoclaving process, while demonstrating broad spectrum sterility effectiveness, also resulted in most notable changes in alginate's key properties. In addition to the specific results with the three sterilization processes and alginate, this study serves as a roadmap to characterize the interrelationships between sterilization processes, fundamental chemical properties, and resulting functional characteristics and processability of hydrogels.

Keywords: Hydrogels, Tissue engineering and regenerative medicine, Biofabrication, Printability, Human adipose-derived stem cells (hASC), Nuclear magnetic resonance spectroscopy

1. Introduction

Sodium alginate is a widely used biomaterial for broad-spectrum biomedical applications including drug delivery, wound healing and tissue engineering¹. It is a naturally occurring copolymer derived from seaweed, and contains 1-4 linked β-D-mannuronic (M) and α-L-guluronic (G) acids forming a long network of polymer chains that mimic the natural ECM topography of human tissues^{2,3}. The length of the chains depends on the molecular weight of the alginate, and there is no definitive sequence for the occurrence of the G and M groups. The carboxylic (R-COOH) and hydroxyl (OH) ions exposed from neighboring uronic acid chains could be bound together through addition of divalent cations such as Ca²⁺ or Ba²⁺, which overall results in the gelation (crosslinking) of the alginate. As a hydrogel, alginate can be utilized for encapsulating cells while isolating them from the host immune response for variegated applications involving cell delivery and protein production^{2,3}. Alginate is also natively non-adherent to the cells and can sustain cells for prolonged periods^{2,3}. This can be desirable for drug testing applications wherein the cellular phenotype/morphology has to be preserved. For tissue engineering applications, alginate can be conjugated with peptides for cellular adhesion, thereby promoting cellular proliferation and ECM production^{4,5}. The chemical crosslinking of the alginate can be synergistically controlled and optimized to render it suitable for use in bioprinting of tissues and organs^{6–9}, which further highlights the versatility of this biopolymer.

The sterility of biomaterials is essential to their function. Sterilization techniques are based on different principles that may utilize heat, chemicals or radiation^{10,11}. Techniques including autoclaving^{12,13}, ethanol washing (EtOH)¹⁴, ultraviolet (UV) exposure^{15,16}, filtering¹³, gamma-irradiation¹⁷ and ethylene oxide (EtO) sterilization¹⁷ have been used for sterilization of alginate in

literature. Of these, autoclaving (heat-based), EtOH (chemical-based) and UV (radiation-based) processes are most widely used, especially in academic research and laboratory settings. This is due to the fact that these are relatively easily accessible, applicable to a wide variety of material formulations, cost effective, and involve simpler safety and processing protocols compared to other methods^{18,19}. It should be noted that EtOH and UV techniques, which are typically used in laboratory settings but not for clinical applications, have been referred to as both disinfection^{20,21} and sterilization^{19,22,23} in literature. For the purpose of simplicity and consistency of terminology, we have referred to these as sterilization in this work.

In autoclaving, the materials are sterilized by exposure to pressurized saturated steam. Autoclaving of liquids, such as the alginate solution used in this study, is typically carried out in a chamber pressurized to 15-18 psi at 121-124°C for 15 min^{24,25}. This results in denaturation of the proteins and enzymes within the microorganisms, thereby leading to their eradication. EtOH sterilization is typically performed by exposing the powder or hydrogel phases of materials to 70% ethanol solution^{19,24}. The ethanol exposure causes coagulation of the proteins and dissolution of the lipids in the cell membranes, which are deleterious to the microorganisms. 70% ethanol solution is preferred over a 100% solution since it evaporates more slowly enabling complete penetration of the reagent and a complete coagulation of the proteins^{20,24}. UV sterilization utilizes non-ionizing UV radiation for denaturing the constituting proteins in the microorganisms. Usually, the 250 nm wavelength UV found in most biosafety cabinets can achieve this at a recommended minimum bulb surface reading of 4.8 mW/cm². In addition to eradicating microorganisms, the intrinsic mechanisms of these sterilization processes also affect the functional properties of the base biopolymers and their subsequent processing.

In this study, we have investigated the effects of autoclaving, EtOH and UV sterilization processes on the chemical, mechanical, printability and biocompatibility characteristics of alginate. Interaction with the thermal fluxes (during autoclaving), chemical reagents (during EtOH exposure) or the free radical generation (during UV irradiation) can alter the constitutive G and M acid content and molecular weight of the alginate by inducing conformational changes or breaking down individual monomers or polymeric chains, thereby significantly affecting subsequent processability and functionality. For example, a change in the ratio of the constitutive monomers (G and M acid) could affect the stiffness of the hydrogel²⁶, while changes to the molecular weight could affect the hydrogel's inherent permeability, stiffness and viscosity^{27–29}. In turn, changes in permeability and stiffness of the hydrogel can be expected to affect nutrient transport and cellular responses^{2,3}. Changes in viscosity would affect the printability of alginate³⁰.

2. Materials and Methods

Figure 1 provides an overview of the sample preparation, sterilization, and subsequent functionality assessment protocols. First, the effectiveness of autoclaving, EtOH and UV processes in sterilizing alginate at different bacterial loads was determined. Then, the effects of the three sterilization processes on alginate monomeric content (G and M acid), molecular weight (number average and weight average), and polydispersity index were assessed. Next, the dynamic viscosity of the three sterilized solutions and compressive stiffness of their hydrogels were determined. This was followed by characterization of their extrusion printability. Finally, the viability and metabolic activity of human adipose-derived stem cells (hASC) in the three groups was assessed over 7 days in culture.

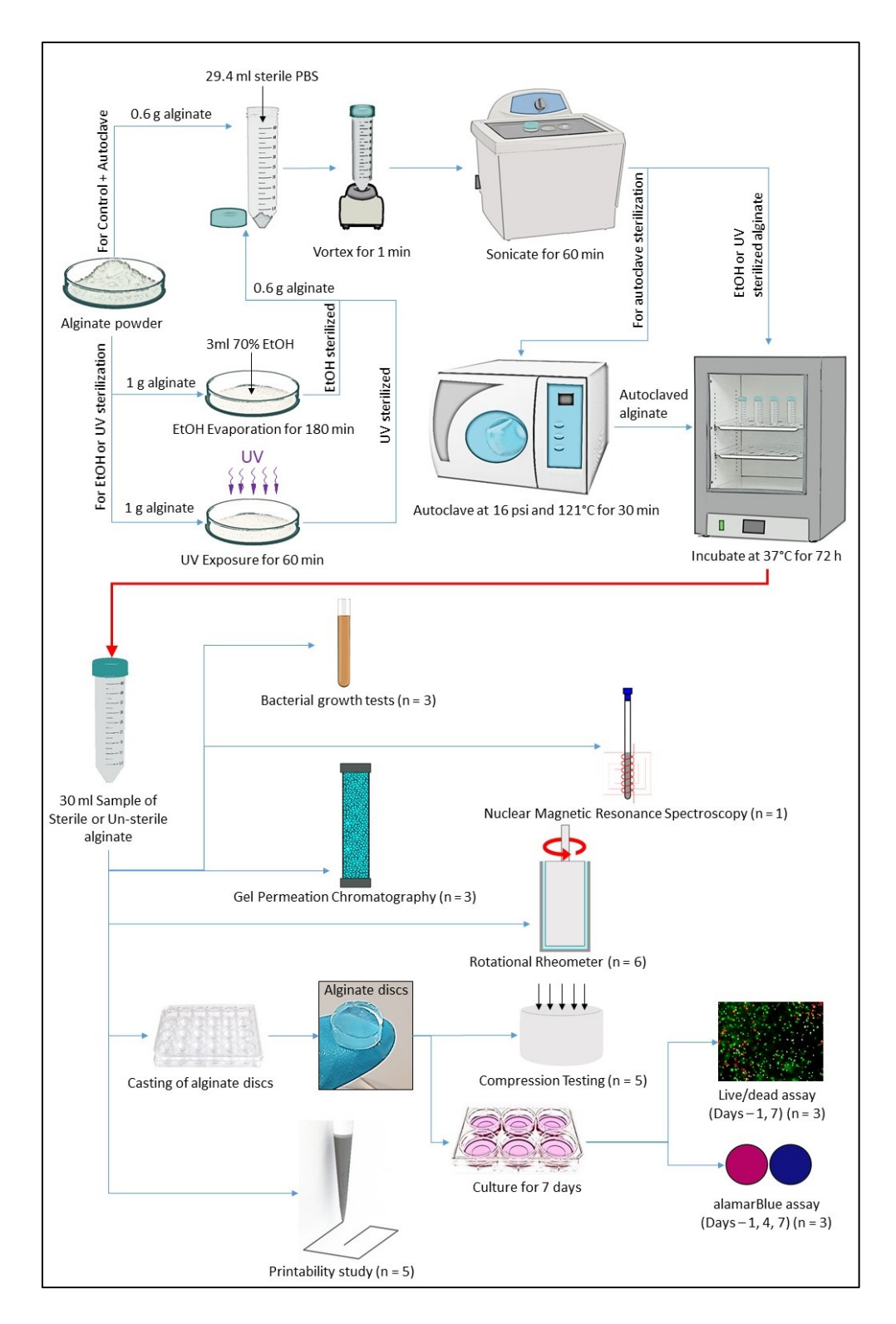


Figure 1. Overview of the experimental studies to determine the effect of autoclaving, EtOH, and UV sterilization on chemical, mechanical, rheological, printability, and biocompatibility characteristics of alginate.

2.1. Preparation of control and sterilized alginate samples

Control group alginate solutions of 2% w/v were prepared by mixing 0.6 g of unsterilized sodium alginate powder (non-sterile grade, Manugel® GMB, Dupont, Wilmington, DE) into 29.4 ml of sterile phosphate buffered saline (PBS; Sigma Aldrich, St. Louis, MO) and vortexing for 1 min followed by sonication for 60 min.

The autoclaved samples were prepared by autoclaving the unsterilized 2% w/v alginate solution at 121°C and 16 psi for 15 min (BioClave 16, Benchmark Scientific Inc, Sayreville, NJ).

To prepare samples of the EtOH group, 1 g of alginate powder was homogeneously dispersed within a petri dish and completely wetted with 3 ml of 70% EtOH (Fisher Scientific, Hampton, NH) for 3 h to allow the ethanol to evaporate. Then, 0.6 g of the EtOH sterilized powder was mixed into 29.4 ml of sterile PBS and vortexed for 1 min followed by sonication for 60 min to constitute the 2% w/v EtOH sterilized alginate solution.

To prepare samples of the UV group, 1 g of alginate powder homogeneously dispersed within a petri dish was exposed to 250 nm UV light inside a Class IIa biosafety cabinet (8 mW/cm², Thermo Fisher Scientific, Waltham, MA) for 1 h. Then, 0.6 g of the UV sterilized powder was mixed into 29.4 ml of sterile PBS and vortexed for 1 min followed by sonication for 60 min to obtain the UV sterilized alginate solution.

Each formulation of alginate was incubated at 37°C for 72 h to ensure homogeneity prior to further testing.

2.2. Assessment of alginate sterility

First, the sterility of aseptically prepared samples devoid of any external bacterial loading was tested to establish a baseline for the material as obtained from the manufacturer. Towards this, 100 µl of sterilized alginate solutions of each of the three test groups were dispensed in 3 ml of sterile tryptic soy broth (TSB; Thermo Fisher Scientific) and incubated for 4 days (n = 3 per group). At day 4, the optical density of the TSB samples was examined at 600 nm in a spectrophotometer (Biospectrophotometer, Eppendorf, Hamburg, Germany). TSB samples without alginate served as the blank controls.

Next, the effectiveness of the sterilized alginate groups in response to different loads (10^8 , 10^6 , 10^4 CFU/ml) of Gram-positive (*Enterococcus faecalis*) and Gram-negative (*Escherichia coli*) bacteria was assessed. Stock solutions for both bacteria in PBS at the three concentrations were prepared beforehand. For samples in the EtOH and UV groups (n = 3 per group), 1 g of alginate powder was inoculated with $100 \mu l$ of the bacterial stock solutions prior to sterilization, and the sterilized powder was used to prepare the 2% w/v solution as previously described. For the autoclaved and control groups, $30 \mu l$ of unsterilized $2\% \mu l$ w/v alginate solutions were inoculated with $100 \mu l$ of the bacterial stock solutions ($n = 3 \mu l$ per group). The relevant set of samples was then autoclaved as previously described. The sterilized and control groups were analyzed for bacterial growth in TSB as described above.

2.3. Nuclear magnetic resonance spectroscopy analysis

For each sterilized and control group, 500 µl of the 2% w/v alginate solution was added to an Eppendorf tube (ThermoFisher Scientific) and frozen at -20°C for 2 h prior to lyophilization. The

solution was then lyophilized in a freeze-dryer (FreeZone 2.5, Labconco, Kansas City, MO) at 2 x 10⁻⁵ N/mm² and -50 °C. This yielded 10 mg of lyophilized alginate polymer. High-resolution ¹H nuclear magnetic resonance spectroscopy (¹H NMR) was performed on 800 μl of the analyte contained in NMR tubes (Wilmad Lab Glass, Vineland, NJ). To prepare the analyte, 800 μl of 99.9% purity deuterium water (D₂O) (Sigma Aldrich) was added to the lyophilized alginate powder and gently pipetted to prepare a homogeneous suspension of 10 mg of alginate in D₂O. This analyte was analyzed in an NMR spectrometer (Avance Neo 600 MHz NMR, with RT BBO Smart Probe and TXI 1H-13C/15N- 2H Probe, Bruker, Billerica, MA) at high temperature (90°C) with water (trace solvent impurity) peak suppression to derive the NMR spectrum. The spectra for all samples were visualized in TopSpin software (4.0.6, Bruker) and the solvent residual peak positions were re-calibrated as per established literature, to accommodate the shift towards higher ppm caused due to the high temperature analysis³¹. The relative G and M content were derived by comparing the derived spectra to the expected spectra in the region of interest as per ASTM standard on analysis of alginate using ¹H NMR³².

2.4. Gel permeation chromatography analysis

For gel permeation chromatography (GPC) analysis, 30 ml of the sterilized and control 2% w/v alginate samples (n = 3 per group) were prepared using previously described protocols, but with 0.1M NaNO₃ as the solvent instead of PBS. After a 3-day incubation period, aliquots of the sample were added to a dilution solution in NaNO₃ to yield a concentration of 0.2% w/v recommended for optimal GPC measurements. Then, 50 µl samples were analyzed in a GPC system (2695 Separations Module, Alliance System, Waters Corp, Milford MA) with PEO/G standard (Agilent Technologies, Shropshire, UK). The number average molecular weight (M_n), weight average

molecular weight (M_w) and polydispersity index $(PI = M_w/M_n)$ were then determined from the GPC chromatograms of the samples.

2.5. Rheological analysis

For each sterilized and control group, 10 ml aliquots of the 2% w/v alginate solution (n = 6 per group) were tested individually in a programmable rheometer (MCR-302, Anton Paar, Graz, Australia). During each test, the alginate sample was subjected to increasing shear rates from 0.1 to 1000 s⁻¹ while maintaining the chamber temperature at 37°C. As alginate is a non-Newtonian fluid, the apparent or effective dynamic viscosity of alginate (Pa.s) was determined from the plot of viscosity vs. shear rate by fitting the Cross model (equation 1)³³. Note that the Cross model is more appropriate for higher concentrations (> 1% w/v) of alginate³⁴ than the more conventional power law model³⁵ for determining apparent viscosity.

$$\eta = \frac{\eta_0}{(1 + (\lambda \dot{\gamma})^m)} \tag{1}$$

where η_0 is the apparent dynamic viscosity at low shear rates (Pa.s), λ is the time constant (s), $\dot{\gamma}$ is the shear rate (s⁻¹) and m is a dimensionless constant. To compare the effects of sterilization processes on the dynamic viscosity, the corresponding viscosity values at low shear rates $(\eta_0)^{34}$ were considered.

2.6. Determination of compressive stiffness

For each sterilized and control group, alginate discs (\emptyset 15.6 mm \times 5.2 mm thick, n = 5 per group) were prepared by casting the 2% w/v alginate solution and serially crosslinking in a custom mold made of a flexible resin (Smooth Cast[®] 300, Smooth-On Inc., Macungie, PA). First, 1 ml of alginate was added to each mold cavity, and 2 ml of 0.1% CaCl₂ solution was introduced to initiate

cross-linking. After 10 minutes, the supernatant was extracted and 0.5% of CaCl₂ solution added. After 20 and 30 minutes, 1% and 2% w/v CaCl₂ solution were added, respectively, following the supernatant aspiration at each step. Finally, after 10 mins of exposure to 2% w/v CaCl₂, the fully crosslinked discs were gently extracted from the mold and stored in PBS for 3 h until testing. This sequential increase of CaCl₂ concentration was necessary to gradually increase the crosslinking density within the hydrogels, thereby minimizing any warpage due to rapid crosslinking⁶.

Samples were tested in an unconfined compression mode following a previously published testing protocol³⁶ on a universal testing system (5944, Instron, Norwood, MA) with a 5 N load cell. The motion of the load cell was controlled through the machine software (Bluehill, Instron, Norwood, MA) in its "Compressive Extension" mode. Briefly, the first cycle comprised of determining the compressive elastic (ramp) modulus by straining the sample at a rate of 0.1 mm/s until 10% strain was reached. The subsequent cycle held the achieved 10% strain constantly for 1000 s for stress relaxation within the discs. Next, cyclical loading varying between 9% and 11% strain at 0.1 mm/s was applied to determine the dynamic modulus of the alginate discs.

2.7. Printability analysis

To evaluate the printability of each sterilized group, 3 ml alginate solution was loaded into the extrusion head of a commercial bioprinter (BioX, Cellink, Sweden) with a 25 G nozzle. Non-sterilized controls were not included in this study as they have limited relevance to actual 3D bioprinted medical applications. The layer height was set at 0.3 mm, and a pre-programmed pattern was printed onto a petri dish with uniformly sprayed 4% CaCl₂ solution at different levels of pressure (4, 6, 8, 10 kPa) and speed (6, 8, 10 mm/s) (n = 5 per group). Images of the printed strands

were then captured using a digital camera (EOS 80D, Canon, Tokyo, Japan) and assessed for print fidelity using a custom MATLAB protocol (Figure S1 of the Supporting Information). For the quantitative characterization of fidelity, two metrics established in literature were used³⁷ – number of discontinuities and spreading ratio (ratio of strand width to the nozzle diameter). Screening experiments were performed to determine and eliminate the combinations of pressure and speed that resulted in extremely poor printability before proceeding to the factorial experiments. Refer to Supporting Information for the MATLAB protocol.

2.8. Cell viability and metabolic activity assays

Cellular viability and metabolic activity assays were performed on crosslinked alginate discs (Ø 15.6 mm × 5.2 mm thick) with human adipose-derived stem cells (hASC) over 7 days of *in vitro* culture. Towards this, hASC (StemProTM R7788115, Thermo Fisher Scientific, Waltham, MA) were cultured in T-75 flasks (NuncTM Easy FlaskTM, Thermo Fisher Scientific) with MesenPRO RSTM basal medium, growth supplement (Thermo Fisher Scientific) and 1% L-Glutamine (Thermo Fisher Scientific). Media changes were performed every 48 h. At 80% confluency, the cells were passaged using 0.25% Trypsin-EDTA (Sigma Aldrich), followed by centrifugation at 100 g for 6 min to create a cell pellet. The cells were then re-constituted in sterilized or unsterilized alginate at 5 × 10⁵ cells/ml by gently pipetting to formulate the bioink.

Alginate discs were cast as previously described and transferred to 6-well plates with 4 ml of hASC media and incubated (37°C, 5% CO₂) for 7 days. Media changes were performed every 24 h. The analyses at day 1 were carried out after 3 h of incubation to allow the cells to recover from previous processing steps³⁸.

For determining cell viability, the discs (n = 3 per group) were subject to LIVE/DEAD® assay (Life Technologies, Carlsbad, CA) at days 1 and 7. Briefly, the hASC media from the cultured discs was aspirated and 1 ml of PBS containing 0.5 µl calcein AM and 2 µl EthD-I was added on top of the discs, followed by 15 min of incubation. Subsequently, the discs were imaged using a fluorescence microscope (DM5500B, Leica Microsystems, Wetzlar, Germany) to determine the cellular viability.

For determining metabolic activity of the cells, the discs (n = 3 per group) were subject to alamarBlue[®] (aB) assay (Thermo Fisher Scientific) and readings taken at days 1, 4 and 7. An acellular control disc was included alongside the cellular discs for normalization of the aB readings. During each reading, media in the 6-well plates containing the cellular and acellular discs was replaced with 4 ml of fresh media containing 10% v/v of the aB reagent. After 4 h, three 1 ml samples from each well were transferred to a 24-well plate and analyzed for absorbance at 570 nm and 600 nm excitation and emission wavelengths, respectively, using a micro-plate reader (Tecan, Männedorf, Switzerland). The absorbance data was reported as % aB reduction after normalizing to the acellular control.

2.9. Statistical analysis

Significance of the effect of treatment factors was determined using two-way ANOVA (molecular weight, dynamic viscosity, compressive stiffness, cell viability and metabolic activity) or three-way ANOVA (printability) with Tukey post-hoc tests in JMP® (SAS, Cary, NC) at a significance level of $\alpha = 0.05$.

3. Results and discussion

3.1. Effectiveness of sterilization processes

Results of the microbial growth tests on non-contaminated alginate samples demonstrated the absence of bacterial growth ($A_{600} = 0.0$ compared to pure TSB samples). These results signify that the non-sterile grade alginate powder obtained from the manufacturer was devoid of microbial contaminants, and the corresponding alginate preparation and handling procedures were aseptic.

To simulate scenarios in which the alginate powder could get contaminated during its manufacturing process or due to non-aseptic preparation or handling protocols, sterility assessment tests were also performed on samples inoculated with different loads of E. faecalis and E. coli. The results are summarized in Figure 2. The interaction effect of the sterilization process and initial bacterial load was significant (p < 0.001). Autoclaving was effective in sterilizing alginate, irrespective of the bacteria type or load. In contrast, the effectiveness of the EtOH and UV sterilization processes was dependent on the bacteria type and the load. The UV process was effective on samples containing E. faecalis irrespective of the load. Against E. coli, the UV process was effective in sterilizing samples loaded at 10^4 and 10^6 CFU/ml, but not at 10^8 CFU/ml. Among the three sterilization processes, EtOH was the least efficacious in that only the samples containing 10^4 CFU/ml of E. coli could be successfully sterilized.

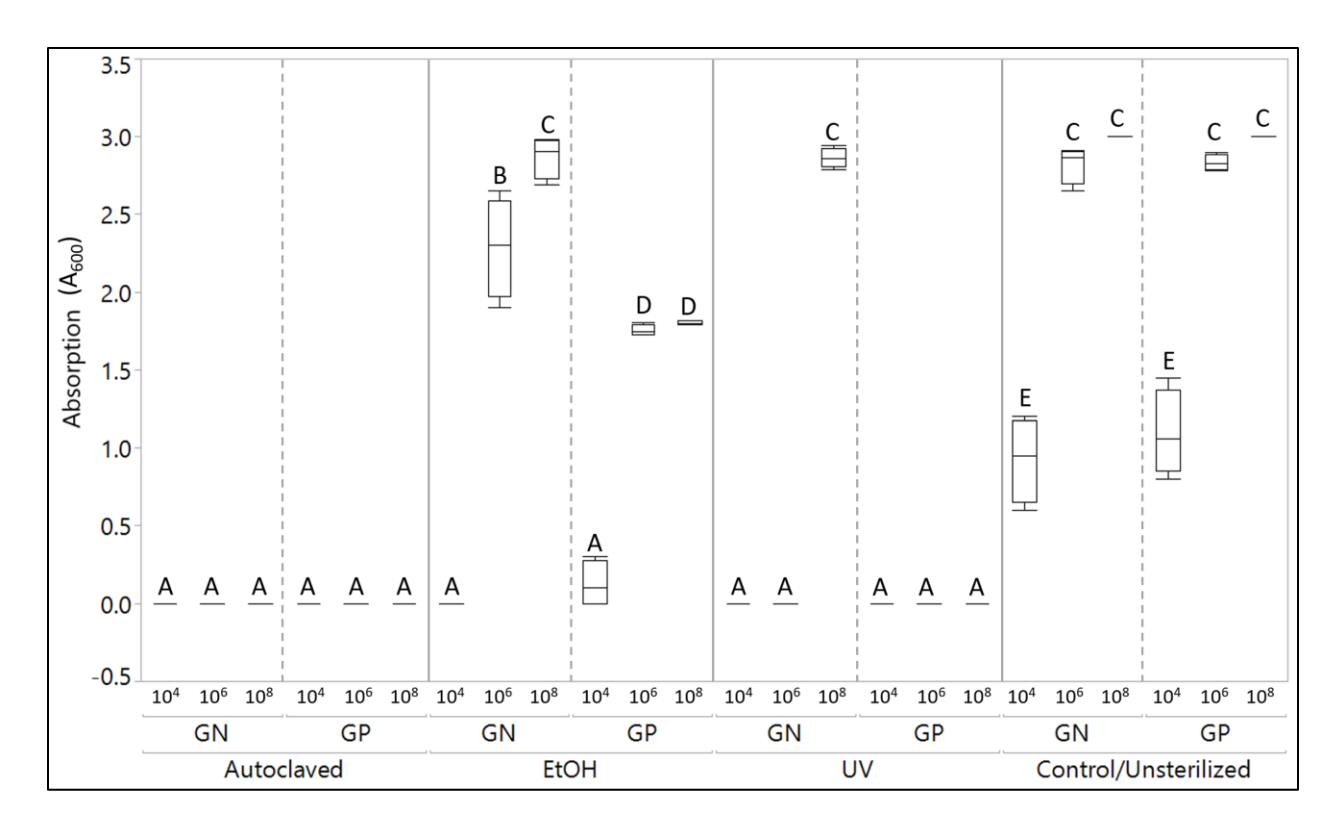


Figure 2. Results of sterility assessment tests on samples inoculated with E. faecalis (Grampositive) and E. coli (Gram-negative) at loads of 10^4 , 10^6 and 10^8 CFU/ml (n = 3 per group). The letters A – E denote groups that were significantly different from each other (p < 0.05) as determined from post hoc tests. Autoclaving demonstrated broad spectrum effectiveness against both bacteria at all three loads, while EtOH was the least effective among the three, demonstrating significant effectiveness only against 10^4 CFU/ml of E. coli. UV exposure process was effective against all samples except E. coli at 10^8 CFU/ml.

3.2. Effect of sterilization processes on the chemical structure of alginate

The NMR spectra shown in Figure 3 demonstrates that the control (unsterilized) and sterilized alginate monomers constituted a high M acid content^{39,40} (M/G > 1). The corresponding G and M acid contents were calculated by integrating the area under the designated peaks in Figure 3 and inputting them in equations (2) and (3) as per the ASTM standard³².

$$G = 0.5(A + C + 0.5(B1+B2+B3))$$
 (2)

$$M = B4 + 0.5(B1+B2+B3)$$
 (3)

Where A, B1, B2, B3, B4 and C represent the areas under the peaks corresponding to the hydrogen atoms in alginate monomers⁴⁰. From this, the % G and M contents were derived as per equations (4) and (5), respectively.

$$%G = 100G/(G+M)$$
 (4)

$$\%M = 100M/(G+M)$$
 (5)

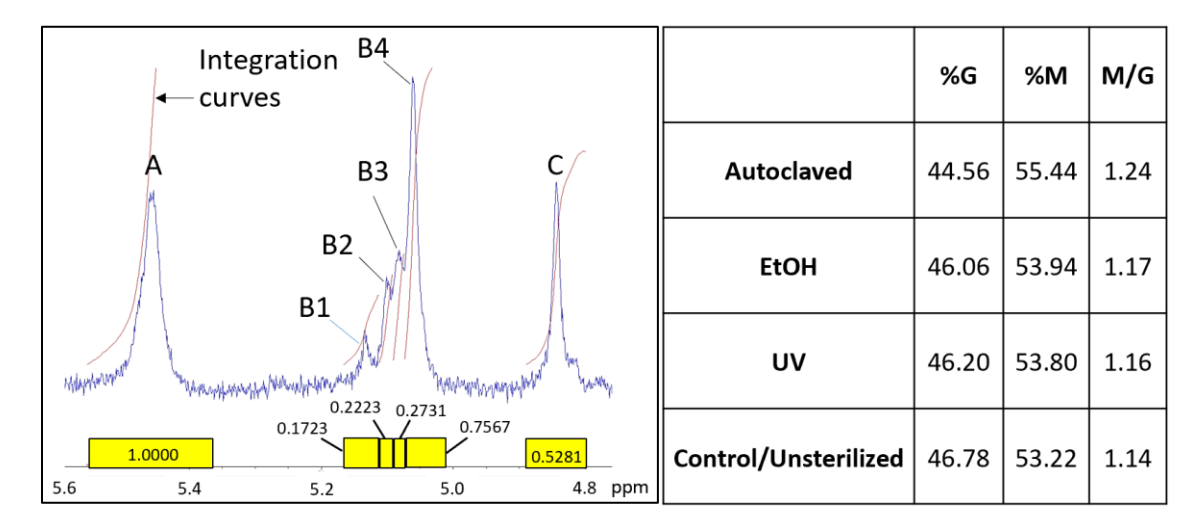


Figure 3. The NMR spectra of the alginate (left) corresponded well with the M-acid rich alginate 40 , which indicated that it may form a softer gel upon gelation. Monomer contents (right) amongst different groups are closely correlated (within $\pm 10\%$) 41 , indicating negligible change due to sterilization.

The M/G ratio as well as the corresponding M and G content in each sterilized group was similar to the unsterilized control. As such, a variation of 10% of the average M/G ratio can be attributed

to error in the least squares approximation in NMR analysis⁴¹. This indicates that the sterilization processes did not significantly affect the inherent monomeric content of the alginate.

3.3. Effect of sterilization processes on the molecular weight and polydispersity of alginate

The effects of sterilization on the molecular weight and polydispersity of alginate are summarized in Figure 4. It is evident that while EtOH and UV sterilization did not affect the molecular weight (p > 0.05), autoclaving resulted in the reduction of both the M_n and M_w (p < 0.0001). This can be attributed to the high thermal fluxes during autoclaving, which facilitate breakdown of longer polymeric chains. Interestingly, autoclaving also resulted in a lower polydispersity index (p < 0.0001), which is a measure of heterogeneity in the sizes of the constitutive molecules. The lower index after autoclaving signifies a narrow molecular size distribution in the solution. This can be attributed to the homogeneous energy (heat and pressure) distribution during autoclaving leading to relatively uniform cleavage of bonds across the polymeric molecules within the alginate.

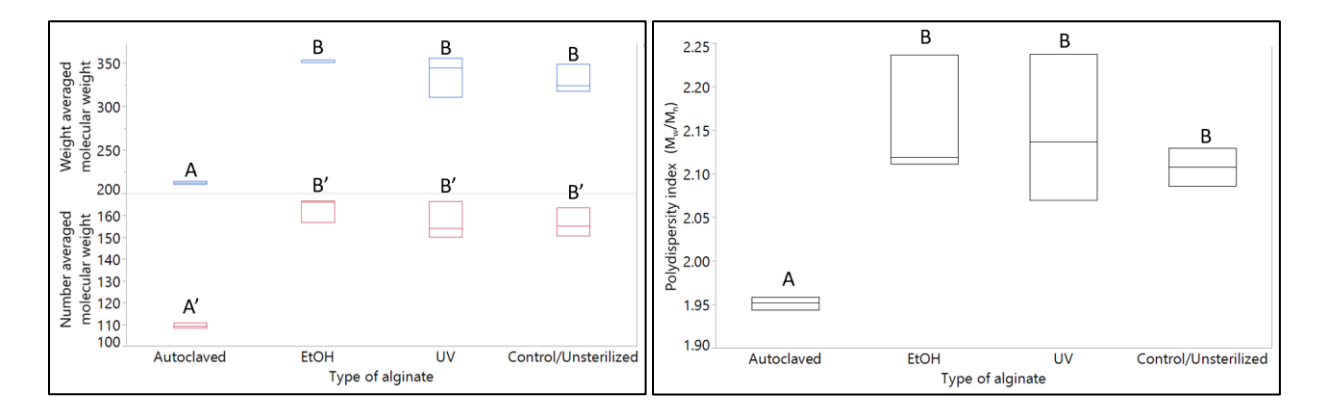


Figure 4. Number average and weight average molecular weights (left) and polydispersity indices (right) of alginate solutions before and after sterilization (n = 3 per group). Groups denoted by A and B (or A' and B') were significantly different from each other (p < 0.05). Of the three

sterilization processes, only autoclaving resulted in a significant reduction in M_n , M_w and polydispersity index (p < 0.0001).

3.4. Effect of sterilization processes on the viscosity of alginate

Figure 5 summarizes the dynamic viscosity of all tested groups at 0.1 s^{-1} shear rate. The EtOH and UV processes did not affect the alginate viscosity (p > 0.05). However, autoclaving resulted in a significant reduction in viscosity (p < 0.0001). This correlates with the reduction in molecular weight of the sample noted earlier^{1,42}. A reduction in the molecular weight indicates smaller lengths of the polymer chains which would otherwise intertwine and lead to a reduction in flowability (increase in viscosity) of the alginate solution.

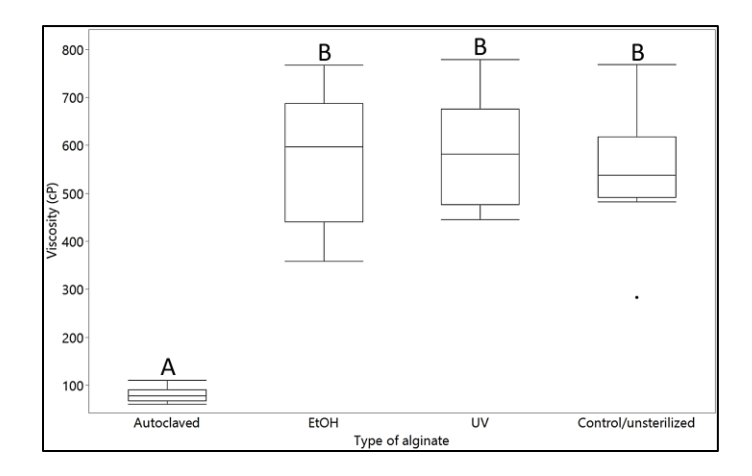


Figure 5. Dynamic viscosities of the three sterilized and one control alginate solution groups at 0.1 s^{-1} shear rate (n = 6 per group). The groups denoted by A and B were significantly different from each other (p < 0.05). Autoclaving resulted in a significantly lower viscosity compared to all other groups (p < 0.0001).

3.5. Effect of sterilization processes on the compressive stiffness of alginate

The ramp and dynamic moduli in compression of alginate hydrogels are presented in Figure 6. For each group, the mean dynamic moduli were higher than mean ramp moduli. This is consistent with prior work demonstrating an increased stiffness of alginate hydrogels under cyclical loading³⁶. It was evident that none of the sterilization processes affected the ramp and dynamic moduli significantly (p > 0.05). This is interesting because a decrease in molecular weight typically results in lower stiffness of hydrogels^{1,27}. However, in case of alginate, the hydrogel stiffness at a given concentration is highly dependent upon the monomer (G or M acid) content⁴² or extent of ionic crosslinking density²⁷. The NMR analysis above had indicated that the monomeric content was similar across all groups, which could partly explain the lack of significant differences in moduli. The gelation kinetics, which are governed by the ionic crosslinker, could also affect the hydrogel stiffness^{27,43}. The relatively rapid gelation kinetics associated with the CaCl₂ crosslinker could result in a gradient of crosslinking density^{27,43} wherein the core of the hydrogel could be more crosslinked than the peripheral regions. The effects of rapid gelation kinetics can potentially mask any subtle differences in hydrogel stiffness that may arise from the differences in molecular weights. In future, the gelation kinetics could be improved (i.e., made more uniform) by finetuning the sequential crosslinking protocols with CaCl₂ or by using slower crosslinkers (e.g., CaCO₃, CaSO₄) that could create more homogeneously crosslinked hydrogels⁴³.

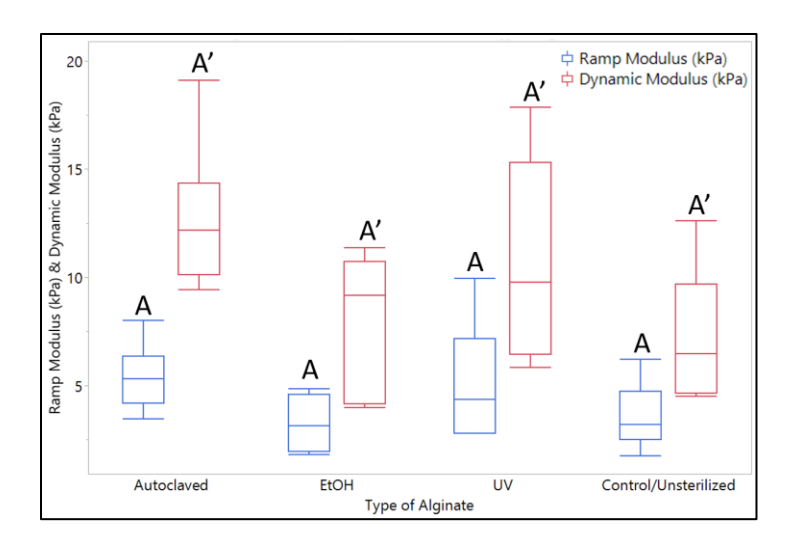
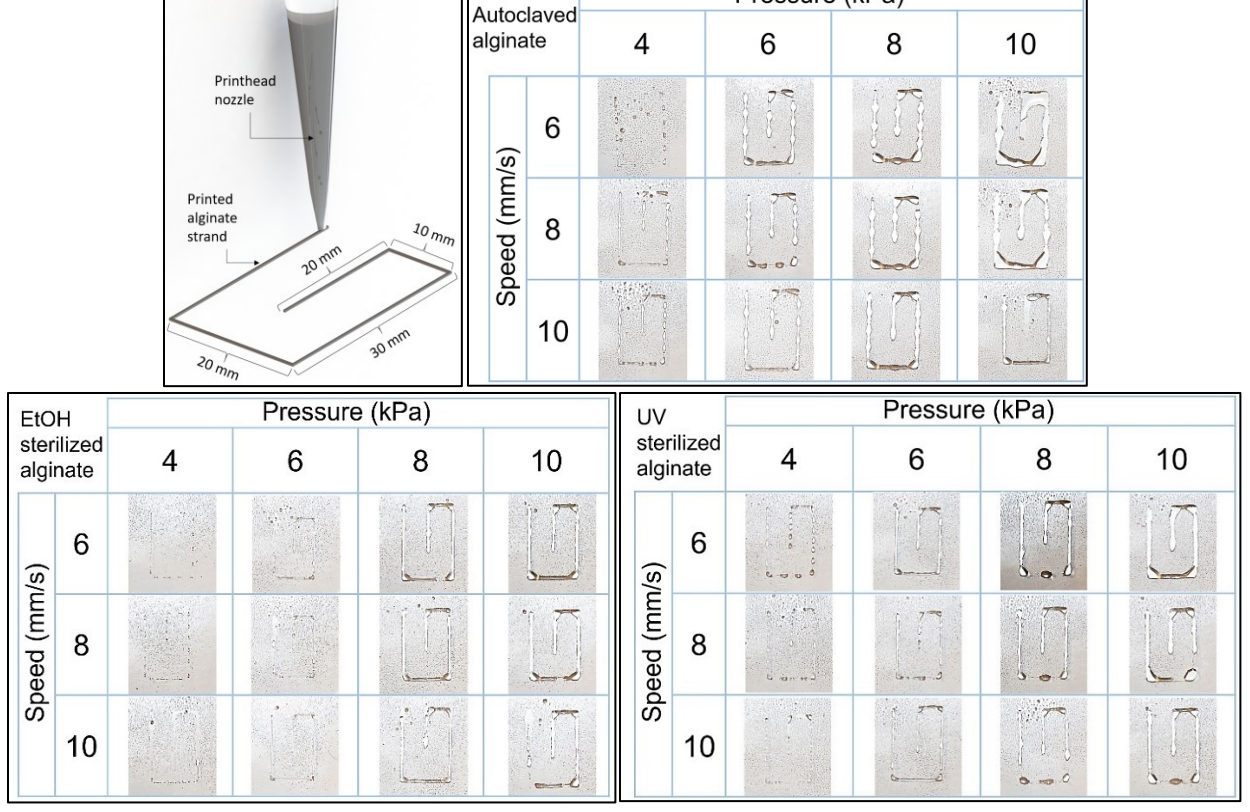


Figure 6. Ramp and dynamic moduli in compression of the three sterilized and one control group of alginate hydrogel (n = 5 per group). All groups denoted by A (ramp modulus) or A' (dynamic modulus) were not significantly different from each other (p > 0.05). The moduli of alginate were not significantly affected by the three sterilization processes.

3.6. Effect of sterilization processes on the printability characteristics of alginate

Figure 7 shows representative printed strand patterns during the screening experiments with all combinations of pressure and speed for the three sterilized alginate groups. The 4 kPa extrusion pressure resulted in consistently poor fidelity across all alginate groups and was therefore excluded from further analysis of printability.



Pressure (kPa)

Figure 7. Representative images from screening experiments to characterize the extrusion printability of the three sterilized alginate solution groups as per the pre-programmed strand pattern (top left) at combinations of four printing pressures and three speeds (n = 5 per group). Printability was consistently poor at 4 kPa, which is why this group was excluded from quantitative analyses.

The results of the three-way ANOVA for the number of discontinuities and spreading ratio are presented in Figure 8. The number of discontinuities were significantly affected by the interaction of the sterilized alginate type and pressure (p < 0.001) and the interaction of the speed and pressure (p < 0.05). Across alginate groups, there were more discontinuities at lower pressure and higher speed, wherein slower extrusion of the hydrogel from the nozzle coupled with a rapid nozzle traversal speed leads to pinching of the hydrogel in contact with the substrate. Post-hoc differences between different sterilized alginate groups printed using the same set of process parameters were

not significant (p > 0.05). Based on these results, we recommend printing each type of sterilized alginate at moderately higher pressures and speeds to achieve high fidelity structures with a minimum number of discontinuities.

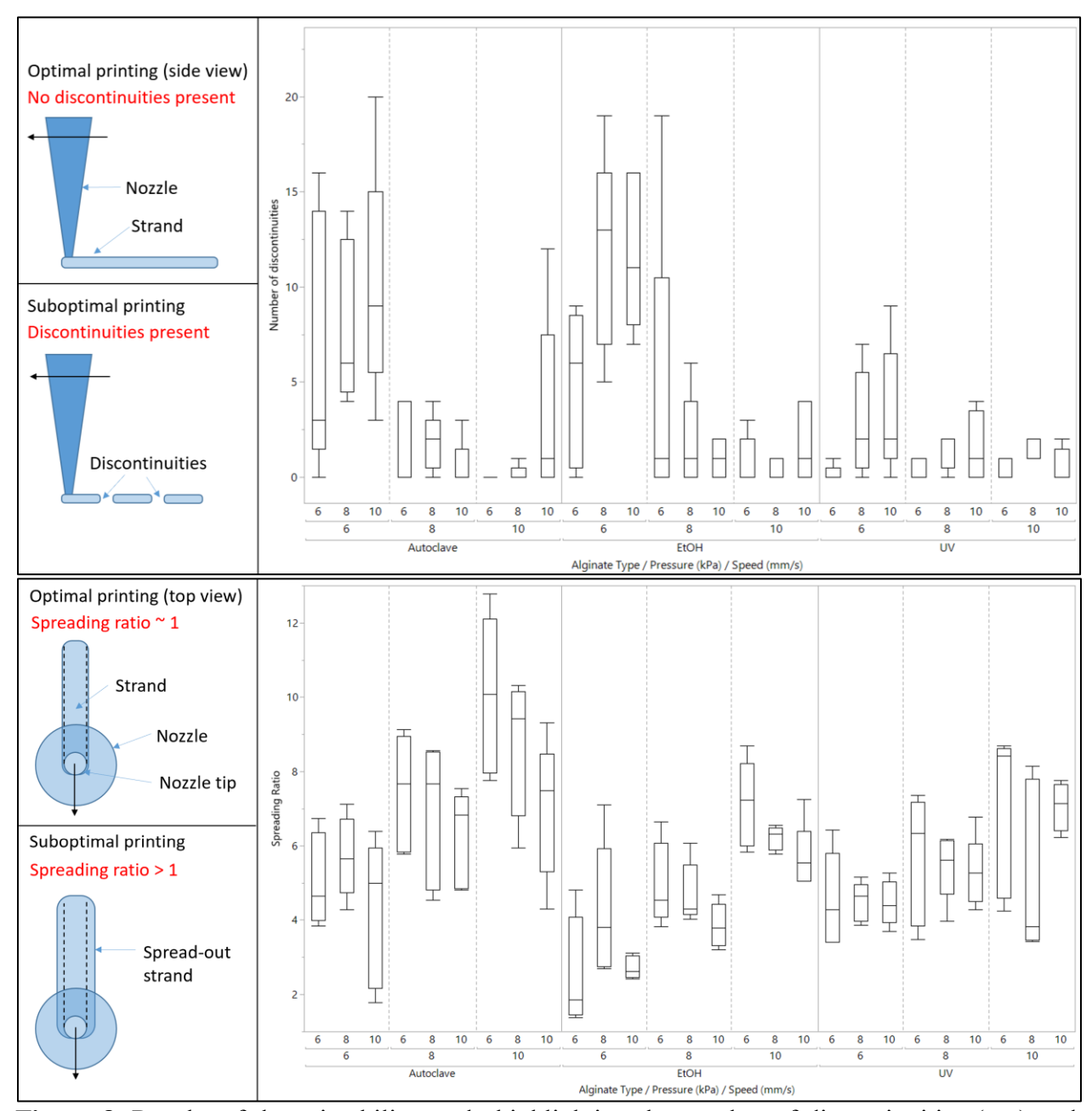


Figure 8. Results of the printability study highlighting the number of discontinuities (top) and spreading ratio (bottom) for the three sterilized alginate groups (n = 5 per group) at the different

combinations of pressure and speed. The interactions of sterilized alginate type and pressure (p < 0.001) and speed and pressure (p < 0.05) significantly affected the number of discontinuities. The spreading ratio was affected by the alginate type (p < 0.001), speed (p < 0.05) and pressure (p < 0.001).

The spreading ratio was affected by the sterilized alginate type (p < 0.001), speed (p < 0.05), and pressure (p < 0.001). Due to the observed reduction in viscosity, the spreading ratios were higher for the autoclaved group for each pressure and speed combination. The spreading ratios were also higher at higher pressures or higher speeds. Since the global minima of the spreading ratios is approximately 2 (i.e. > 1), it is evident that there is an intrinsic flowability to each alginate group. As such, a spreading ratio closer to 1 could be achieved in future studies by increasing the crosslinker or alginate concentration 27,29 .

Note that the 2% w/v concentration used in this study and by others^{6,43–45} is towards the lower end of the typical range of alginate concentrations used in extrusion bioprinting, and the printability characteristics can be expected to vary by concentration. Printability could also be affected by the ionic crosslinker and the crosslinking protocols (e.g., introducing the crosslinker coaxially or as a mist^{46,47}). Furthermore, printability could also be assessed for other printing methods such as inkjet printing⁴⁸.

3.7. Effect of sterilization processes on the viability and metabolic activity of encapsulated cells in alginate

Representative Live/Dead images from days 1 and 7 and the results of aB analysis for days 1, 4 and 7 for the three sterilized alginate groups are presented in Figure 9. The viability of hASC consistently remained high (\geq 90%) across all groups over a week in culture. Results of the ANOVA showed that the viability was significantly affected by the time point (p < 0.001) but not by the sterilized alginate type or their interaction (p > 0.05). Results of aB analysis show that the metabolic activity of the cells was significantly affected by the sterilized alginate type (p < 0.01) but not by the time point or their interaction (p > 0.05). At each time point, the metabolic activity was highest for the autoclaved group and lowest for the UV group. The high metabolic activity in the autoclaved group at each time point could be attributed to the significant decrease in alginate's molecular weight due to the heat-based process. The lower molecular weight leads to increased matrix permeability⁴⁹, degradation rate, and deformability over time²⁸, thereby facilitating better nutrient and waste exchange during in vitro culture.

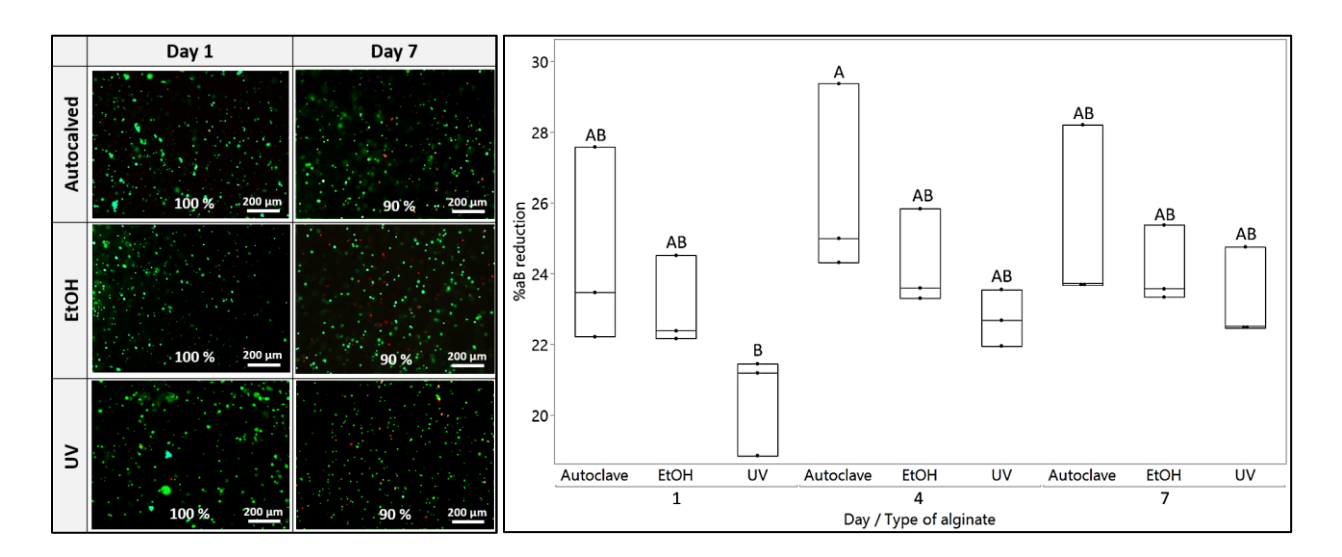


Figure 9. Live/Dead[®] images (left) of the sterilized and control alginate groups at day 1 and 7 (n = 3 per group), and aB assay results (right) at days 1, 4, and 7 (n = 3 per group). The viability was primarily affected by the time point (p < 0.0001) whereas the metabolic activity was primarily

affected by the sterilized alginate type (p < 0.01). Groups denoted by A or B were significantly different from each other (p < 0.05), but not different from AB groups.

Looking at the results holistically, autoclaving was most effective in ensuring sterility of alginate. Autoclaving reduced the molecular weight of alginate, thereby impacting its rheology (lower viscosity), printability (higher spreading ratio) and biological properties (higher metabolic activity), while yielding a highly consistent solution as indicated by the low polydispersity index. These results are in agreement with a prior study in which alginate hydrogel properties including swelling ratio, and storage and loss moduli were found to be significantly affected by autoclaving but not by EtOH or UV exposure⁵⁰. Another investigation on the effects of UV exposure and autoclaving on alginate powders did not report any significant changes to the monomeric content of the alginate, and noted that autoclaving reduced the alginate molecular weight, which is consistent with our observations⁵¹. Interestingly, they also reported a reduction in molecular weight due to UV exposure, which is in contrast to our observations. This difference can be attributed to the higher exposure intensity used in that study (approximately 30 mW/cm² compared to the 8 mW/cm² used in this work). This highlights that for a given sterilization process, the processing conditions can affect the material properties differently. Furthermore, each sterilization process could have vastly different effects on different materials. For example, autoclaving was found to not affect the molecular weight of methylcellulose⁵² in contrast to the reduction in alginate molecular weight reported in this and prior studies^{50,51}.

In future, relevant functional characteristics of autoclaved alginate could be optimized by appropriately tuning the composition of the starting solution and processing parameters. For

example, using a higher molecular weight alginate⁴² or higher w/v concentration of the starting solution would lead to higher viscosity of sterilized solution and yield high fidelity printed features. Print fidelity of the different compositions can be optimized by appropriately fine-tuning printing parameters including the extrusion pressure and print speed. Different crosslinking strategies such as partial or complete gelation of the extruded filament through coaxial extrusion⁴⁶ or misting⁴⁷ of crosslinker ions can also be investigated and optimized. In addition, other characteristics such as hydrogel stiffness could be enhanced by using a crosslinker with slower gelation kinetics^{27,43}, increasing G acid content or molecular weight of alginate by choosing the appropriate seaweed source and its grade⁴², or higher concentration of the initial solution²⁷. To facilitate long-term storage, one recommendation would be to lyophilize the autoclaved alginate. The lyophilized powder could be reconstituted into the concentration relevant for the application at the time of use.

Whereas this study focused on autoclaving, EtOH, and UV sterilization processes, other sterilization methods including filter, EtO, and gamma irradiation have also been utilized in literature^{19,24}. These methods too, can affect the biomaterial properties. For example, filter sterilization can reduce the solution viscosity by filtering out the longer polymeric chains⁵³, EtO can leave carcinogenic residues⁵⁴, and gamma radiation can cleave polymeric chains⁵⁵, thereby affecting the molecular weight and mechanical properties^{55,56}. The framework presented in this study can be used to investigate the effects of these other sterilization process on alginate and other hydrogels in the future.

4. Conclusion

The effects of three widely available sterilization processes – autoclaving, EtOH, and UV – on important functional characteristics of alginate were investigated in this study. Among the three processes, autoclaving proved to be the most effective in achieving sterility in samples contaminated with both Gram-positive and Gram-negative bacteria in loads as high as 10⁸ CFU/ml, while EtOH was the least effective. The G and M acid content of the alginate remained relatively unchanged after each sterilization process, but autoclaving significantly reduced the molecular weight, and in turn, the dynamic viscosity of the alginate solution. Interestingly, autoclaving also yielded a highly monodisperse alginate solution which could have practical significance, if utilized appropriately. None of the sterilization processes affected the compressive stiffness of the alginate hydrogels significantly, which could be attributed to the similar monomeric content in the three groups. All alginate hydrogel groups demonstrated good viability of encapsulated hASC after one week of in vitro culture, but the autoclaved group demonstrated the highest cellular metabolic activity, likely due to increased permeability resulting from the lower molecular weight. The effects of autoclaving on viscosity were also reflected in the printability results, in that the spreading ratio of autoclaved alginate was higher than the other groups. Furthermore, across the three sterilized groups, strands printed at moderate pressures and speeds consistently resulted in a lower number of discontinuities and lower spreading ratio. The approach and methods used in this study can be extended to investigate the characteristics of other sterilization processes or other biomaterials in the future. This study can serve as a roadmap to guide researchers to make informed decisions in selecting the appropriate sterilization process and processing parameters that best suit the biomaterial and its application.

Supporting Information

Figure S1 and MATLAB code to analyze alginate strand printability.

Acknowledgements

The authors acknowledge the financial support from the US National Science Foundation (CMMI-1652489) and NC State College of Engineering's Research Experience for Undergraduates (REU) program. They also thank Dr. Siddhartha "Sid" Thakur and Ms. Lyndy Bleu Harden from NC State's College of Veterinary Medicine for providing support for the sterility assessment experiments.

References

- Lee, K. Y.; Mooney, D. J. Alginate: Properties and Biomedical Applications. *Prog. Polym. Sci.* 2012, 37 (1), 106–126.
 https://doi.org/10.1016/J.PROGPOLYMSCI.2011.06.003.
- (2) Andersen, T.; Strand, B. L.; Formo, K.; Alsberg, E.; Christensen, B. E. Alginates as Biomaterials in Tissue Engineering. In *Carbohydrate Chemistry: Chemical and Biological Approaches*; Rauter, A. P., Lindhorst, T. K., Eds.; RSC Publications: London, 2011; pp 227–258. https://doi.org/10.1039/9781849732765-00227.
- (3) Ma, P. X. Alginate for Tissue Engineering. 2005, 24–36.https://doi.org/10.1201/9781420027563-5.
- (4) Shachar, M.; Tsur-Gang, O.; Dvir, T.; Leor, J.; Cohen, S. The Effect of Immobilized RGD Peptide in Alginate Scaffolds on Cardiac Tissue Engineering. *Acta Biomater.* **2011**, *7* (1), 152–162. https://doi.org/10.1016/J.ACTBIO.2010.07.034.
- (5) Yu, J.; Du, K. T.; Fang, Q.; Gu, Y.; Mihardja, S. S.; Sievers, R. E.; Wu, J. C.; Lee, R. J.

- The Use of Human Mesenchymal Stem Cells Encapsulated in RGD Modified Alginate Microspheres in the Repair of Myocardial Infarction in the Rat. *Biomaterials* **2010**, *31* (27), 7012–7020. https://doi.org/10.1016/J.BIOMATERIALS.2010.05.078.
- (6) Chansoria, P.; Narayanan, L. K.; Schuchard, K.; Shirwaiker, R. A. Ultrasound-Assisted Biofabrication and Bioprinting of Preferentially Aligned Three-Dimensional Cellular Constructs. *Biofabrication* 2019, 11 (3), 14861. https://doi.org/10.1088/1758-5090/ab15cf.
- (7) Jovic, T. H.; Kungwengwe, G.; Mills, A. C.; Whitaker, I. S. Plant-Derived Biomaterials: A Review of 3D Bioprinting and Biomedical Applications. *Front. Mech. Eng.* 2019, 5, 19. https://doi.org/10.3389/fmech.2019.00019.
- (8) Chansoria, P.; Shirwaiker, R. 3D Bioprinting of Anisotropic Engineered Tissue Constructs with Ultrasonically Induced Cell Patterning. *Addit. Manuf.* 2020, 32, 101042. https://doi.org/10.1016/j.addma.2020.101042.
- (9) Xu, T.; Zhao, W.; Zhu, J. M.; Albanna, M. Z.; Yoo, J. J.; Atala, A. Complex Heterogeneous Tissue Constructs Containing Multiple Cell Types Prepared by Inkjet Printing Technology. *Biomaterials* 2013, 34 (1), 130–139. https://doi.org/10.1016/j.biomaterials.2012.09.035.
- (10) Dai, Z.; Ronholm, J.; Tian, Y.; Sethi, B.; Cao, X. Sterilization Techniques for Biodegradable Scaffolds in Tissue Engineering Applications. *J. Tissue Eng.* 2016, 7, 204173141664881. https://doi.org/10.1177/2041731416648810.
- (11) Russell, Hugo & Ayliffe's Principles and Practice of Disinfection, Preservation and Sterilization; Fraise, A. P., Maillard, J.-Y., Sattar, S., Eds.; Wiley-Blackwell, 2013.
- (12) Duggirala, S.; Deluca, P. P. Rheological Characterization of Cellulosic and Alginate Polymers. *PDA J. Pharm. Sci. Technol.* **1996**, *50* (5), 290–296.

- (13) Wong, M.; Siegrist, M.; Wang, X.; Hunziker, E. Development of Mechanically Stable Alginate/Chondrocyte Constructs: Effects of Guluronic Acid Content and Matrix Synthesis. J. Orthop. Res. 2001, 19 (3), 493–499. https://doi.org/10.1016/S0736-0266(00)90023-8.
- (14) Naghieh, S.; Sarker, M. D.; Abelseth, E.; Chen, X. Indirect 3D Bioprinting and Characterization of Alginate Scaffolds for Potential Nerve Tissue Engineering Applications. J. Mech. Behav. Biomed. Mater. 2019, 93, 183–193. https://doi.org/10.1016/j.jmbbm.2019.02.014.
- (15) Liakos, I.; Rizzello, L.; Bayer, I. S.; Pompa, P. P.; Cingolani, R.; Athanassiou, A.
 Controlled Antiseptic Release by Alginate Polymer Films and Beads. *Carbohydr. Polym.*2013, 92 (1), 176–183. https://doi.org/10.1016/j.carbpol.2012.09.034.
- (16) Eroğlu, M.; Kurşaklioğlu, H.; Misirli, Y.; Iyisoy, A.; Acar, A.; Işin Doğan, A.; Denkbaş, E. B. Chitosan-Coated Alginate Microspheres for Embolization and/or Chemoembolization: In Vivo Studies. *J. Microencapsul.* 2006, 23 (4), 367–376. https://doi.org/10.1080/02652040500286318.
- (17) Leo, W. J.; McLoughlin, A. J.; Malone, D. M. Effects of Sterilization Treatments on Some Properties of Alginate Solutions and Gels. *Biotechnol. Prog.* 1990, 6 (1), 51–53. https://doi.org/10.1021/bp00001a008.
- (18) Galante, R.; Pinto, T. J. A.; Colaço, R.; Serro, A. P. Sterilization of Hydrogels for Biomedical Applications: A Review. *J. Biomed. Mater. Res. Part B Appl. Biomater.* **2018**, *106* (6), 2472–2492. https://doi.org/10.1002/jbm.b.34048.
- (19) Dai, Z.; Ronholm, J.; Tian, Y.; Sethi, B.; Cao, X. Sterilization Techniques for Biodegradable Scaffolds in Tissue Engineering Applications. *J. Tissue Eng.* **2016**, 7,

- 2041731416648810. https://doi.org/10.1177/2041731416648810.
- (20) Block, S. S. *Disinfection, Sterilization, and Preservation*; Lippincott Williams & Wilkins, 2001.
- (21) Vogt, L.; Rivera, L. R.; Liverani, L.; Piegat, A.; El Fray, M.; Boccaccini, A. R. Poly(ε-Caprolactone)/Poly(Glycerol Sebacate) Electrospun Scaffolds for Cardiac Tissue Engineering Using Benign Solvents. *Mater. Sci. Eng. C* 2019, 103, 109712. https://doi.org/10.1016/j.msec.2019.04.091.
- (22) Evrova, O.; Kellenberger, D.; Scalera, C.; Calcagni, M.; Giovanoli, P.; Vogel, V.; Buschmann, J. Impact of UV Sterilization and Short Term Storage on the in Vitro Release Kinetics and Bioactivity of Biomolecules from Electrospun Scaffolds. *Sci. Rep.* 2019, 9 (1), 1–11. https://doi.org/10.1038/s41598-019-51513-1.
- (23) R, G.; C, P.; H, D.; P, C.; N, D. G.; R, C.; R, M. Effects of Different Sterilization Methods on the Physico-Chemical and Bioresponsive Properties of Plasma-Treated Polycaprolactone Films. *Biomed. Mater.* 2017, 12 (1), 015017–015017. https://doi.org/10.1088/1748-605X/AA51D5.
- (24) Galante, R.; Pinto, T. J. A.; Colaço, R.; Serro, A. P. Sterilization of Hydrogels for Biomedical Applications: A Review. *J. Biomed. Mater. Res. Part B Appl. Biomater.* **2018**, 106 (6), 2472–2492. https://doi.org/10.1002/jbm.b.34048.
- (25) Lerouge, S.; Simmons, A. *Sterilisation of Biomaterials and Medical Devices*; Woodhead Publishing: Sawston, 2012.
- (26) Wong, M. Alginates in Tissue Engineering. In *Biopolymer Methods in Tissue Engineering*; Humana Press: New Jersey, 2004; pp 77–86. https://doi.org/10.1385/1-59259-428-X:77.

- (27) Freeman, F. E.; Kelly, D. J. Tuning Alginate Bioink Stiffness and Composition for Controlled Growth Factor Delivery and to Spatially Direct MSC Fate within Bioprinted Tissues. *Sci. Rep.* **2017**, *7* (1). https://doi.org/10.1038/s41598-017-17286-1.
- (28) Kong, H. J.; Kaigler, D.; Kim, K.; Mooney, D. J. Controlling Rigidity and Degradation of Alginate Hydrogels via Molecular Weight Distribution. *Biomacromolecules* **2004**, *5* (5), 1720–1727. https://doi.org/10.1021/bm049879r.
- (29) Li, J.; Illeperuma, W. R. K.; Suo, Z.; Vlassak, J. J. Hybrid Hydrogels with Extremely High Stiffness and Toughness. *ACS Macro Lett.* **2014**, *3* (6), 520–523. https://doi.org/10.1021/mz5002355.
- (30) Jia, J.; Richards, D. J.; Pollard, S.; Tan, Y.; Rodriguez, J.; Visconti, R. P.; Trusk, T. C.; Yost, M. J.; Yao, H.; Markwald, R. R.; Mei, Y. Engineering Alginate as Bioink for Bioprinting. *Acta Biomater.* 2014, 10 (10), 4323–4331.
 https://doi.org/10.1016/J.ACTBIO.2014.06.034.
- (31) Gottlieb, H. E.; Kotlyar, V.; Nudelman, A. NMR Chemical Shifts of Common Laboratory Solvents as Trace Impurities. **1997**. https://doi.org/10.1021/JO971176V.
- (32) ASTM Standard F2259 10. Standard Test Method for Determining the Chemical Composition and Sequence in Alginate by Proton Nuclear Magnetic Resonance (1 H NMR) Spectroscopy. ASTM Int. West Conshohocken, PA, 2003 2012. https://doi.org/10.1520/F2259-10R12E01.
- (33) Cross, M. M. Rheology of Non-Newtonian Fluids: A New Flow Equation for Pseudoplastic Systems. *J. Colloid Sci.* **1965**, *20* (5), 417–437. https://doi.org/10.1016/0095-8522(65)90022-X.
- (34) Wang, L.; Zhu, F.; Lu, D. Rheological Properties of Sodium Alginate and Xanthan Pastes

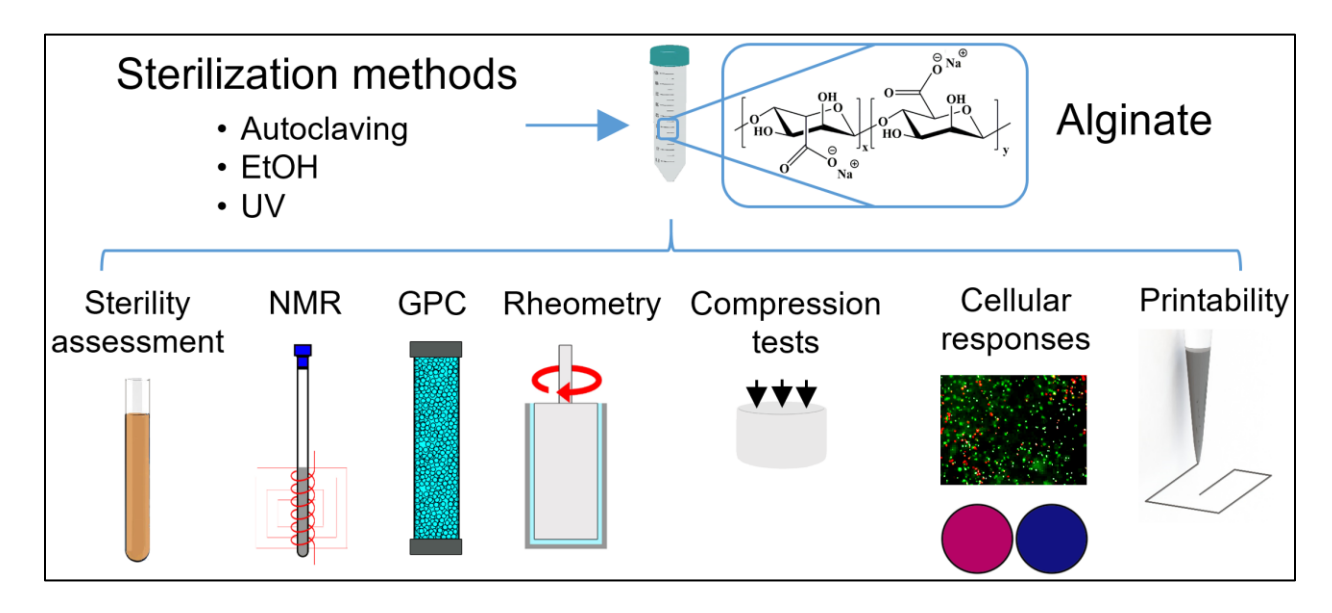
- on Cotton with Reactive Dye in Screen Printing. *Text. Res. J. 83* (17), 1873–1884. https://doi.org/10.1177/0040517513481873.
- (35) Rezende, R. A.; Bártolo, P. J.; Mendes, A.; Filho, R. M. Rheological Behavior of Alginate Solutions for Biomanufacturing. *J. Appl. Polym. Sci.* **2009**, *113* (6), 3866–3871. https://doi.org/10.1002/app.30170.
- (36) Fisher, M. B.; Henning, E. A.; Söegaard, N. B.; Dodge, G. R.; Steinberg, D. R.; Mauck, R. L. Maximizing Cartilage Formation and Integration via a Trajectory-Based Tissue Engineering Approach. *Biomaterials* 2014, 35 (7), 2140–2148. https://doi.org/10.1016/j.biomaterials.2013.11.031.
- (37) Chen, D. X. B. Extrusion Bioprinting of Scaffolds. In Extrusion Bioprinting of Scaffolds for Tissue Engineering Applications; Springer International Publishing, 2019; pp 117– 145. https://doi.org/10.1007/978-3-030-03460-3_6.
- (38) Chansoria, P.; Shirwaiker, R. Characterizing the Process Physics of Ultrasound-Assisted Bioprinting. *Sci. Rep.* **2019**, *9* (1), 13889. https://doi.org/10.1038/s41598-019-50449-w.
- (39) ASTM Standard F2064 17. Standard Guide for Characterization and Testing of Alginates as Starting Materials Intended for Use in Biomedical and Tissue Engineered Medical Product Applications https://compass.astm.org/EDIT/html_annot.cgi?F2064+17 (accessed Apr 7, 2019).
- (40) Jensen, H. M.; Larsen, F. H.; Engelsen, S. B. Characterization of Alginates by Nuclear Magnetic Resonance (NMR) and Vibrational Spectroscopy (IR, NIR, Raman) in Combination with Chemometrics. *Methods Mol. Biol.* 2015, *1308*, 347–363. https://doi.org/10.1007/978-1-4939-2684-8_22.
- (41) Castellano, S.; Bothner-By, A. A. Analysis of NMR Spectra by Least Squares. J. Chem.

- Phys. 1964, 41 (12), 3863–3869. https://doi.org/10.1063/1.1725826.
- (42) Fu, S.; Thacker, A.; Sperger, D. M.; Boni, R. L.; Buckner, I. S.; Velankar, S.; Munson, E. J.; Block, L. H. Relevance of Rheological Properties of Sodium Alginate in Solution to Calcium Alginate Gel Properties. *AAPS PharmSciTech* 2011, 12 (2), 453–460. https://doi.org/10.1208/s12249-011-9587-0.
- (43) Kuo, C. K.; Ma, P. X. Ionically Crosslinked Alginate Hydrogels as Scaffolds for Tissue Engineering: Part 1. Structure, Gelation Rate and Mechanical Properties. *Biomaterials* 2001, 22 (6), 511–521. https://doi.org/10.1016/S0142-9612(00)00201-5.
- (44) Khalil, S.; Sun, W. Bioprinting Endothelial Cells with Alginate for 3D Tissue Constructs. *J. Biomech. Eng.* **2009**, *131* (11). https://doi.org/10.1115/1.3128729.
- (45) Narayanan, L. K.; Huebner, P.; Fisher, M. B.; Spang, J. T.; Starly, B.; Shirwaiker, R. A.; Fitts, E. P. 3D-Bioprinting of Polylactic Acid (PLA) Nanofiber—Alginate Hydrogel Bioink Containing Human Adipose-Derived Stem Cells. *ACS Biomater. Sci. Eng.* **2016**, *2* (10), 1732–1742. https://doi.org/10.1021/acsbiomaterials.6b00196.
- (46) Gao, Q.; He, Y.; Fu, J. zhong; Liu, A.; Ma, L. Coaxial Nozzle-Assisted 3D Bioprinting with Built-in Microchannels for Nutrients Delivery. *Biomaterials* **2015**, *61*, 203–215. https://doi.org/10.1016/j.biomaterials.2015.05.031.
- (47) MacCallum, B.; Naseri, E.; Butler, H.; MacNevin, W.; Tasker, R. A.; Ahmadi, A.
 Development of a 3D Bioprinting System Using a Co-Flow of Calcium Chloride Mist.
 Bioprinting 2020, e00085. https://doi.org/10.1016/j.bprint.2020.e00085.
- (48) Delaney, J. T.; Liberski, A. R.; Perelaer, J.; Schubert, U. S. Reactive Inkjet Printing of Calcium Alginate Hydrogel Porogens A New Strategy to Open-Pore Structured Matrices with Controlled Geometry. *Soft Matter* **2010**, *6* (5), 866–869.

- https://doi.org/10.1039/b922888h.
- (49) Andersson, H.; Hjärtstam, J.; Stading, M.; von Corswant, C.; Larsson, A. Effects of Molecular Weight on Permeability and Microstructure of Mixed Ethyl-Hydroxypropyl-Cellulose Films. *Eur. J. Pharm. Sci.* 2013, 48 (1–2), 240–248. https://doi.org/10.1016/J.EJPS.2012.11.003.
- (50) Stoppel, W. L.; White, J. C.; Horava, S. D.; Henry, A. C.; Roberts, S. C.; Bhatia, S. R. Terminal Sterilization of Alginate Hydrogels: Efficacy and Impact on Mechanical Properties. *J. Biomed. Mater. Res. Part B Appl. Biomater.* 2014, 102 (4), 877–884. https://doi.org/10.1002/jbm.b.33070.
- (51) Yu, H.; Cauchois, G.; Schmitt, J. F.; Louvet, N.; Six, J. luc; Chen, Y.; Rahouadj, R.; Huselstein, C. Is There a Cause-and-Effect Relationship between Physicochemical Properties and Cell Behavior of Alginate-Based Hydrogel Obtained after Sterilization? *J. Mech. Behav. Biomed. Mater.* 2017, 68, 134–143. https://doi.org/10.1016/j.jmbbm.2017.01.038.
- (52) Hodder, E.; Duin, S.; Kilian, D.; Ahlfeld, T.; Seidel, J.; Nachtigall, C.; Bush, P.; Covill, D.; Gelinsky, M.; Lode, A. Investigating the Effect of Sterilisation Methods on the Physical Properties and Cytocompatibility of Methyl Cellulose Used in Combination with Alginate for 3D-Bioplotting of Chondrocytes. *J. Mater. Sci. Mater. Med.* 2019, 30 (1), 1–16. https://doi.org/10.1007/s10856-018-6211-9.
- Vandenbossche, G. M. R.; Remon, J.-P. Influence of the Sterilization Process on Alginate Dispersions. *J. Pharm. Pharmacol.* **1993**, *45* (5), 484–486. https://doi.org/10.1111/j.2042-7158.1993.tb05582.x.
- (54) Rutala, W. A.; Weber, D. J. Low-Temperature Sterilization Technologies: Do We Need to

- Redefine " Sterilization & quot; ? *Infect. Control Hosp. Epidemiol.* **1996**, *17* (2), 87–91. https://doi.org/10.2307/30141007.
- (55) Lee, D. W.; Choi, W. S.; Byun, M. W.; Park, H. J.; Yu, Y. M.; Lee, C. M. Effect of γ-Irradiation on Degradation of Alginate. *J. Agric. Food Chem.* 2003, 51 (16), 4819–4823. https://doi.org/10.1021/jf021053y.
- (56) Nguyen, H.; Morgan, D. A. F.; Forwood, M. R. Sterilization of Allograft Bone: Effects of Gamma Irradiation on Allograft Biology and Biomechanics. *Cell Tissue Bank.* **2007**, *8* (2), 93–105. https://doi.org/10.1007/s10561-006-9020-1.

For Table of Contents Use Only



Manuscript title: Effects of autoclaving, EtOH and UV sterilization on the chemical, mechanical, printability and biocompatibility characteristics of alginate

Authors: Parth Chansoria, Lokesh Karthik Narayanan, Madison Wood, Claudia Alvarado, Annie Lin, and Rohan A. Shirwaiker